A COMPARISON OF JPDA AND BELIEF PROPAGATION FOR DATA ASSOCIATION IN SSA

Mark Rutten,[*] Jason Willams[*,†] and Neil Gordon[*,‡]
[*] *NSID, Defence Science and Technology Organisation, Australia*
[†] *School of EEE, The University of Adelaide, Australia*
[‡] *School of ITEE, The University of Queensland, Australia*

Jason Stauch and Jason Baldwin
Schafer Corporation, USA

Moriba Jah
Space Vehicles Directorate, Air Force Research Laboratory, USA

ABSTRACT

The process of initial orbit determination, or catalogue maintenance, using a set of unlabelled observations requires a method of choosing which observation was due to which object. Realities of imperfect sensors mean that the association must be made in the presence of missed detections, false alarms and previously undetected objects. Data association is not only essential to processing observations, it can also be one of the most significant computational bottlenecks.

The constrained admissible region multiple hypothesis filter (CAR-MHF) is an algorithm for initial orbit determination using short-arc, optical (angles only), observations of space objects. CAR-MHF uses joint probabilistic data association (JPDA), a well-established approach to multi-target data association. A recent development in the target tracking literature is the use of graphical models to formulate data association problems. Using an approximate inference algorithm, belief propagation (BP), on the graphical model results in an algorithm that is both computationally efficient and accurate.

This paper compares association performance on a set of deep-space objects with CAR-MHF using JPDA and BP. The results of the analysis show that by using the BP algorithm there are significant gains in computational load, with negligible loss in accuracy in the calculation of association probabilities.

1. INTRODUCTION

Data association is an essential, but challenging, component of all multiple object tracking algorithms. Where an object may not be seen (due to the characteristics of the object, the sensor or the environment), where false measurements are produced (due to a noisy sensor or other environmental effects) or where there are multiple objects or multiple measurements, there will be ambiguity over which measurements belong to which objects. This association ambiguity needs to be resolved in order to incorporate the measurement information into estimates of the object states.

The constrained admissible region multiple hypothesis filter (CAR-MHF) [1, 2, 3] is an algorithm for initial orbit determination and catalogue maintenance which uses the joint probabilistic data association (JPDA) algorithm [4]. JPDA is a multi-target data association algorithm that generates an association probability for each measurement with each object. This is achieved through exhaustively evaluating the probability of all valid object-to-measurement combinations. The version of JPDA presented in this paper additionally accounts for the mixture of Gaussians describing the probability density of the state of each object within CAR-MHF.

In cases where there are many objects and many measurements the JPDA algorithm can be computationally expensive [5]. There are practical methods, such as gating, which can help to reduce the size of the problems [4]. However for many tracking systems, including CAR-MHF, JPDA remains a computational bottleneck. Approximation methods are required for large problems, where the time needed to explicitly calculate JPDA is impractical. A promising technique for approximating the measurement-to-object association probabilities is the use of belief propagation (BP) within a graphical model of the association problem [6, 7, 8]. In difficult air-defence problems BP has been shown to be much faster than JPDA, while maintaining sufficient accuracy.

This paper aims to extend the analysis of the BP approximation algorithm to orbit determination problems within CAR-MHF.

The structure of this paper is as follows: Section 2 discusses the constrained admissible region (CAR) and filtering with multiple range and range-rate hypotheses (MHF). Section 3 outlines the joint probabilistic data association (JPDA) algorithm within the multiple hypothesis framework. The belief propagation (BP) approximation to JPDA is presented in Section 4. Indicative results from a small simulation are shown in Section 5 with conclusions given in Section 6.

2. CAR-MHF

2.1 The Constrained Admissible Region

The constrained admissible region (CAR) is an area in measured range and range-rate found by constraining both the energy (essentially the duration) and the eccentricity (the shape) of possible orbits [1, 2]. The CAR, as discussed in this paper, relies on the measurement of angles and their rates. Augmenting the angles and angle-rates with feasible ranges and range-rates completes the six-dimensional state required for initial orbit determination giving a set of possible positions and velocities of the orbiting object.

The energy, $\mathcal{E}$, of an orbit can be written in terms of the inertial position, $\mathbf{r}$, and velocity, $\dot{\mathbf{r}}$, of the object through

$$\mathcal{E} = \frac{||\dot{\mathbf{r}}||^2}{2} - \frac{\mu}{||\mathbf{r}||}, \tag{1}$$

where μ is the standard gravitational parameter of Earth. This equation can be rearranged to form a relationship between the measured range and range-rate. The resulting equation [2] produces contours of constant orbital energy as a function of range and range-rate. Similarly, eccentricity, e, is related to angular momentum, $\mathbf{h}$, and specific energy through

$$e = \sqrt{1 + \frac{2\mathcal{E}||\mathbf{h}||^2}{\mu^2}}. \tag{2}$$

Again the equation can be rearranged to form a relationship between the measured range and range-rate resulting in contours of constant eccentricity as a function of range and range-rate.

An example of the two types of constraints is shown in Figure 1. The plot on the left of Figure 1 is the CAR of a simulation from a fictitious sensor located at DSTO Edinburgh observing Optus C1 on 11th July 2014 at 15:45UTC. The plot on the right in Figure 1 shows a more representative CAR for the purposes of initial orbit determination, where the eccentricity and semi-major axis have been constrained to orbits in near-GEO (GEosynchronous Orbit).

2.2 Multiple-Hypothesis Filter

The CAR provides a constrained region of the object state space which is supported by a single measurement. As further measurements are received the object state can be refined with that information. A principled way of approaching this is through recursive state-space estimation. For this application a non-linear filter is required due to the non-linear nature of orbital propagation and the non-linearity of the relationship between the measurements and the orbital state.

The unscented Kalman filter (UKF) [9] is used in this application to propagate the probability distribution of the object over time and refine it with measurement information. While the UKF is typically a computationally efficient and accurate filter it assumes that the probability of the state is Gaussian distributed. In general a CAR, such as that shown on the right in Figure 1, cannot be accurately represented by a Gaussian. To ameliorate this shortcoming a mixture of multiple Gaussians is used to represent a uniform distribution over the CAR to any desired accuracy [2]. This mixture results in a filter which is a bank of many UKFs, one for each hypothesis (component of the mixture). Clever hypothesis management (which is not reviewed in this paper) results in the number of elements in the mixture reducing over time as more measurements refine the location of the object.

Following the derivation of the well-known Gaussian sum filters [10, 11], a multiple-hypothesis filter can be derived which accommodates the Gaussian mixture representation of the CAR. In this paper x_k is used

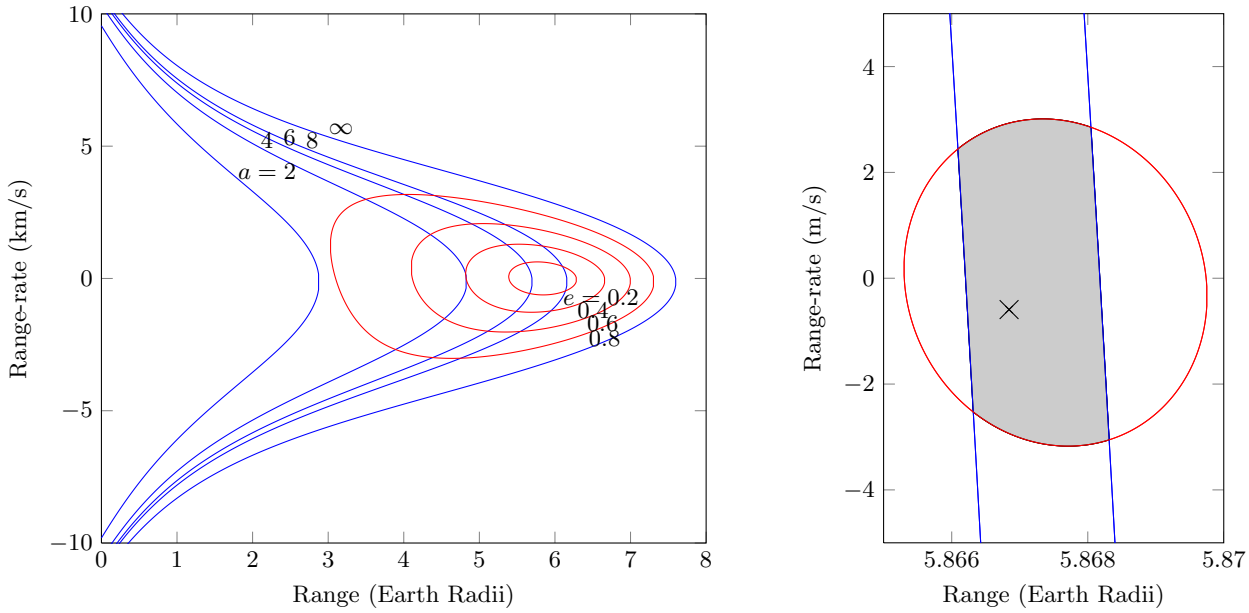

Figure 1: The constrained admissible region (CAR). The figure on the left shows the CAR for several values (Earth radii) of the semi-major axis, a, in blue and eccentricity, e in red. The figure on the right shows the CAR with semi-major axis between 42.15×10^6m and 42.2×10^6m (blue lines) and eccentricity between zero and 10^{-3} (red ellipse). The grey-shaded area is the resulting admissible region and the true range and range-rate of the object is shown by the cross.

to represent the state of the object at time k, z_k is the measurement at time k and Z^k is the history of all measurements $Z^k = \{z_1, \ldots, z_k\}$. The filter follows these steps

Initialisation The probability distribution of the object at time $k-1$ is given by the weighted Gaussian mixture

$$p(x_{k-1}|Z^{k-1}) = \sum_i \alpha^i_{k-1} \mathcal{N}(x_{k-1}; \hat{x}^i_{k-1|k-1}, P^i_{k-1|k-1}), \tag{3}$$

where $\mathcal{N}(x; m, \Sigma)$ represents a Gaussian distribution in variable x with mean m and covariance Σ. The factors α^i_{k-1} represent the weight on each component of the mixture defined such that $\sum_i \alpha^i_{k-1} = 1$.

Prediction The predicted mixture can be written as

$$p(x_k|Z^{k-1}) = \sum_i \alpha^i_{k-1} \mathcal{N}(x_k; \hat{x}^i_{k|k-1}, P^i_{k|k-1}) \tag{4}$$

where $\hat{x}^i_{k|k-1}$ and $P^i_{k|k-1}$ can be calculated using the standard unscented filter formulation, the details of which can be found in [9]. Note that the mixture weights are unchanged in the prediction step.

Update The mixture, updated with a measurement at time k, z_k, can be written as

$$p(x_k|Z^k) = \sum_i \alpha^i_k \mathcal{N}(x_k; \hat{x}^i_{k|k}, P^i_{k|k}) \tag{5}$$

where, $\hat{x}^i_{k|k}$ and $P^i_{k|k}$ can be calculated from the ith predicted component and the measurement at time k using the unscented filtering equations. The updated component weight is given by

$$\bar{\alpha}^i_k = \alpha^i_{k-1} \mathcal{N}(z_k; \hat{z}^i_k, S^i_k) \tag{6}$$

$$\alpha^i_k = \frac{\bar{\alpha}^i_k}{\sum_j \bar{\alpha}^j_k}, \tag{7}$$

where $\hat{z}^i_k$ and S^i_k are the predicted measurement and innovations covariance.

3. JOINT PROBABILISTIC DATA ASSOCIATION IN CAR-MHF

The MHF presented in the previous section assumes that there is a single object and a perfect sensor, that is no false alarms and no missed detections. In a realistic scenario an algorithm must be able to deal with multiple objects, false alarms and missed detections. A data association algorithm, which associates measurements with objects, is used to deal with these practicalities. In this case we use the joint probabilistic data association algorithm (JPDA) [4].

The imperfections of the sensor and it's detection performance are expressed through the probability of detection, P_d and the spatial density of false alarms, λ. The probability of detection is modelled through the characterisation of the sensor and may take into account properties of the object (although that detail is not included in this derivation of the algorithm). The false alarm rate is typically chosen to reflect the performance of the sensor, but is also related to the processing chain that produces detections. In this case the number of false alarms is assumed to be Poisson-distributed.

3.1 Multiple object MHF with association ambiguity

In the remainder of the paper N_k is the number of objects at time k and x_k^t is the state of object t at time k. There are m_k measurements at time k and so now the history of all measurements is $Z^k = \{Z_1, \ldots, Z_k\}$ where $Z_k = \{z_k^1, \ldots, z_k^{m_k}\}$. The probability distribution of the state of object t is represented by

$$p(x_k^t|Z^k) = \sum_{i=1}^{n_k^t} \alpha_k^{i,t} \mathcal{N}(x_k^t; \hat{x}_{k|k}^{i,t}, P_{k|k}^{i,t}) \tag{8}$$

where n_k^t is the number of mixture components representing the probability distribution of object t.

Define $\beta_k^{j,t}$ as the probability that measurement $j \in \{0, 1, \ldots, m_k\}$ is from object t, where $j = 0$ corresponds to the object not being detected. Given $\beta_k^{j,t}$, we can modify the update step of the MHF in the previous section to reflect the ambiguous measurement origin. The mixture updated with a set of measurements at time k can be written as (8) where

$$\alpha_k^{j,i,t} = \alpha_{k-1}^{i,t} \times \begin{cases} P_d \lambda^{-1} \mathcal{N}(z_k^j; \hat{z}_k^{i,t}, S_k^{i,t}) & \text{for } j > 0 \text{ (object detected)} \\ (1 - P_d) & \text{for } j = 0 \text{ (object not detected)} \end{cases} \tag{9}$$

$$w_k^{j,t} = \sum_{i=1}^{n_k^t} \alpha_k^{j,i,t} \tag{10}$$

$$\alpha_k^{i,t} = \sum_{j=0}^{m_k} \frac{\beta_k^{j,t}}{w_k^{j,t}} \alpha_k^{j,i,t} \tag{11}$$

In analogy with the previous section $\hat{z}_k^{i,t}$ and $S_k^{i,t}$ are the predicted measurement and innovations covariance for mixture component i of object t. Here $\alpha_k^{j,i,t}$ is the ith component weight for the jth measurement from the tth object. $w_k^{j,t}$ is the likelihood of measurement j, given that it came from object t. The updated weights are a sum over contributions from each measurement according to the association probabilities $\beta_k^{j,t}$.

In a similar way, $\hat{x}_{k|k}^{i,t}$ and $P_{k|k}^{i,t}$ can be calculated as a weighted sum of contributions from each measurement. An unscented filter gives the mean, $\hat{x}_{k|k}^{j,i,t}$ and covariance, $P_{k|k}^{j,i,t}$, of the updated distribution for each measurement from each component of the mixture from each object

$$p(x_k^{i,t}|z_k^j, Z^{k-1}) = \mathcal{N}(x_k^{i,t}; \hat{x}_{k|k}^{j,i,t}, P_{k|k}^{j,i,t}). \tag{12}$$

In the special $j = 0$ (not detected) case the mean and covariance come from the predicted distribution, $\hat{x}_{k|k}^{0,i,t} = \hat{x}_{k|k-1}^{i,t}$ and $P_{k|k}^{0,i,t} = P_{k|k-1}^{i,t}$. Then the component distribution can be found by summing over contributions from each measurement

$$p(x_k^{i,t}|Z^k) = \sum_{j=0}^{m_k} w_k^{j,i,t} \mathcal{N}(x_k^{i,t}; \hat{x}_{k|k}^{j,i,t}, P_{k|k}^{j,i,t}), \tag{13}$$

where

$$w_k^{j,i,t} = \frac{\beta_k^{j,t}}{w_k^{j,t}} \frac{\alpha_k^{j,i,t}}{\alpha_k^{i,t}} \tag{14}$$

By moment-matching, we can calculate the updated mean and covariance of each component in an object's mixture [4]

$$\hat{x}_{k|k}^{i,t} = \sum_{j=0}^{m_k} w_k^{j,i,t} \hat{x}_{k|k}^{j,i,t} \tag{15}$$

$$P_{k|k}^{i,t} = \sum_{j=0}^{m_k} w_k^{j,i,t} \left[P_{k|k}^{j,i,t} + \left(\hat{x}_{k|k}^{j,i,t} - \hat{x}_{k|k}^{i,t} \right) \left(\hat{x}_{k|k}^{j,i,t} - \hat{x}_{k|k}^{i,t} \right)^T \right]. \tag{16}$$

Note that with the association probabilities $\beta_k^{j,t}$ supplied, the updated distributions above are calculated independently for each object. All dependencies that arise due to the association ambiguity between objects and measurements are captured in the association probabilities. As such the computational complexity of the algorithm outlined in this section is limited to $O(n_k^t m_k)$ for each object.

3.2 Calculation of the association probabilities

There are several methods that could be chosen to calculate the association probabilities $\beta_k^{j,t}$ [8]. CAR-MHF currently uses the joint probabilistic data association (JPDA) algorithm [4], which is outlined here.

For each object $t \in \{1, \ldots, N_k\}$ we define an association variable $a_k^t \in \{0, 1, \ldots, m_k\}$, the value of which is an index to the measurement with which the object is hypothesised to be associated (zero if the object is hypothesised to have not been detected). Then we can define the joint association variable over all N_k objects

$$A_k = \{a_k^1, \ldots, a_k^{N_k}\}. \tag{17}$$

JPDA proceeds by calculating the probabilities

$$P\{A_k | Z^k\} \tag{18}$$

for all feasible associations A_k. The definition of a_k ensures that for a given A_k each object can be associated with a single measurement (or zero). A feasible association must also be constrained such that a measurement can have only one source, that is

$$\sum_{t=1}^{N_k} \delta(a_k^t, j) \leq 1 \quad \forall j > 0, \tag{19}$$

where $\delta(a, b) = 1$ if $a = b$ and 0 otherwise.

Following [4] (with some rearrangement), the posterior probability of a joint association event can be written as

$$P\{A_k | Z^k\} \propto \prod_{t=1}^{N_k} \psi_k^{a_k^t, t}, \tag{20}$$

where $\psi_k^{j,t}$ is given by

$$\psi_k^{j,t} = \begin{cases} P_d \lambda^{-1} f_t \left[z_j(k) \right] & \text{for } j > 0 \\ 1 - P_d & \text{for } j = 0, \end{cases} \tag{21}$$

and $f_t \left[z_j(k) \right]$ is the likelihood of measurement j given that it came from object t. Note the stark similarity between $\psi_k^{j,t}$ in (21) and the weights $\alpha_k^{j,i,t}$ in (9). In fact for the case of a Gaussian mixture ψ should be replaced by w from (10), giving the probability of the joint association event [12]

$$P\{A_k | Z^k\} \propto \prod_{t=1}^{N_k} w_k^{a_k^t, t}. \tag{22}$$

Having calculated the probability of all of the joint events, $P\{A_k|Z^k\}$, the association probabilities can be found as the marginals of the joint distribution. The marginal probability of an association event is given by

$$P\{a_k^t|Z^k\} = \sum_{a_k^{t'}, t' \neq t} P\{a_k^1, \ldots, a_k^{N_k}|Z^k\}, \tag{23}$$

and then

$$\beta_k^{j,t} = P\{a_k^t = j|Z^k\}. \tag{24}$$

4. BELIEF PROPAGATION

It is apparent from the previous section that the computationally complex component of JPDA is the calculation of the marginal association probabilities through the explicit evaluation of the joint association events. JPDA is closely related to the #P-complete problem of calculating the matrix permanent [5]. Gating [4], which involves removing unlikely association hypotheses before computing association probabilities, is one effective measure to reduce the number of joint events, but cannot completely remove the issue. For large problems explicit calculation will be impossible within practical time and memory constraints, so approximations are required. This section presents an approximation to JPDA based on belief propagation (BP) within a directed graph. The BP algorithm was developed in [6], where it was shown that this approximation is both fast and accurate.

The previous section defined the association variables a_k^t, which are an index to the measurement hypothesised for object t. The associations can be equivalently described through $b_k^j \in \{0, 1, \ldots, N_k\}$, for each measurement j, the value of which is an index to the object with which the measurement is hypothesised to be associated (zero if the measurement is hypothesised to be either a false alarm or a new object). The sets of association variables are redundant, that is they exhaustively encode the association hypotheses in complementary ways. Rather than specify the constraints on the association variables a_k^t, given in (19), the BP algorithm considers both sets of association variables and forces consistency between them.

The JPDA algorithm calculates the marginal probabilities, $P\{a_k^t|Z^k\}$, explicitly as outlined in the previous section. The belief propagation algorithm approximates these probabilities as marginals of the joint distribution

$$P\{a_k^1, \ldots, a_k^{N_k}, b_k^1, \ldots, b_k^{m_k}|Z^k\} = \prod_t \left\{ \psi_k^{a_k^t, t} \prod_j \phi_{t,j}(a_k^t, b_k^j) \right\} \tag{25}$$

The factors

$$\phi_{t,j}(a_k^t, b_k^j) = \begin{cases} 0, & a_k^t = j, b_k^j \neq t \text{ or } b_k^j = t, a_k^t \neq j \\ 1, & \text{otherwise} \end{cases} \tag{26}$$

ensure the consistency between the a_k^t and the b_k^j sets of association variables. The $\psi_k^{a_k^t, t}$ are as defined in the previous section and, as before, should be replaced with the relevant sum over terms in the Gaussian mixture. The desired marginals are given by

$$P\{a_k^t|Z^k\} = \sum_{a_k^{t'}, t' \neq t; b_k^j \forall j} P\{a_k^1, \ldots, a_k^{N_k}, b_k^1, \ldots, b_k^{m_k}|Z^k\}. \tag{27}$$

The graphical model used to encode the association variables is shown in Figure 2. The belief propagation algorithm generates messages which are passed between nodes along the edges in the graph. In the case of a tree-structured graph BP is exact, however for a graph which admits cycles, such as Figure 2, BP is necessarily an approximation. The message passing alternates between two sets of messages; those passed from the left to the right (referring to Figure 2), which are written as $(\mu_{a_k^t \to b_k^j})$ then those passed from the right to the left, $(\mu_{b_k^j \to a_k^t})$.

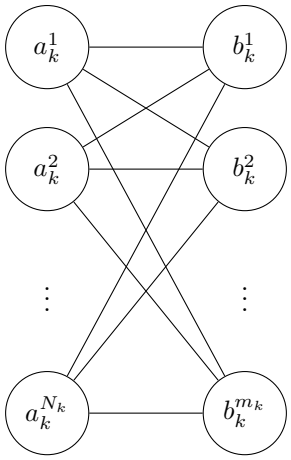

Figure 2: The graphical model used to encode the association variables.

As shown in [7] the message update equations simplify to

$$\mu_{t\to j} = \frac{\psi_k^{j,t}}{1 - P_d + \sum_{j'\neq j, j'>0} \psi_k^{j',t} \mu_{j'\to t}} \tag{28}$$

$$\mu_{j\to t} = \frac{1}{1 + \sum_{j'\neq j, j'>0} \mu_{t'\to j}}, \tag{29}$$

where the notation $(\mu_{t\to j})$ has been used for $(\mu_{a_k^t \to b_k^j})$. Convergence of the algorithm is guaranteed, with a proof presented in [7], and a numerical test for convergence of the algorithm is discussed in [8]. Once the algorithm has converged the approximate marginal probabilities are given by

$$\hat{\beta}_k^{j,t} = \frac{\psi_k^{j,t} \mu_{j\to t}}{\sum_{j'} \psi_k^{j',t} \mu_{j'\to t}}. \tag{30}$$

5. SIMULATION

This section considers a cluster of 26 objects in GEO orbit. The CAR-MHF framework, using the JPDA algorithm of Section 3, is run on a sequence of observations of these objects over several days. In the observation instants where there are two or more objects competing for measurements, the performance of JPDA and BP is compared. A total of 192 association examples result from this simulation. The comparison of the two algorithms is made through both computational cost and accuracy of the association probabilities, $\beta_k^{j,t}$. In the following results the computational cost has been normalised by the lowest execution time of the JPDA algorithm.

In this simulation CAR-MHF uses a false alarm intensity, $\lambda = 100$, and the probability of detection, $P_d = 0.95$. The number of false measurements is of the order of 1 or 2 per scan, with the relatively high false alarm intensity resulting from the precision of the measurements. It should be noted that low false alarm rate and high probability of detection conditions are where the BP algorithm performance is weakest [7]. As P_d increases and λ decreases the BP algorithm decreases in accuracy and increases in compute time.

Figure 3 shows the histograms of the (normalised) computation cost for both JPDA and BP algorithms on the same 192 association examples. It is immediately apparent that the BP algorithm is not only quicker than the JPDA algorithm, but its run-time is more consistent. The total run-time of the JPDA is 2870, while the total run-time of the BP algorithm is 130, indicating that BP is roughly twenty times faster, on average. While Figure 3 shows the distributions over compute times, it does not indicate the relative speed of the algorithms on specific examples. Figure 4 shows the ratio of the JPDA compute time, T_J, to the BP compute time, T_B, for each example, $r = T_J/T_B$, so values $r > 1$ imply that BP is faster, while $r < 1$ imply BP is slower. It is apparent that for the vast majority of the examples BP is significantly faster than JPDA, but

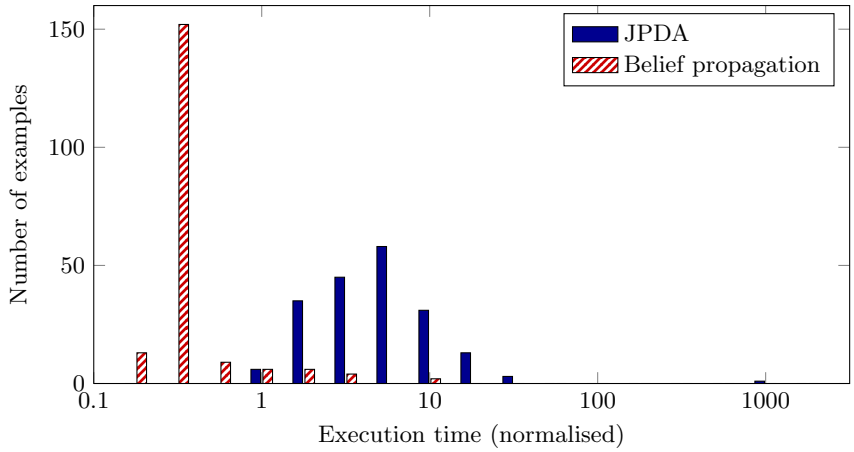

Figure 3: Histograms comparing the compute time (normalised to the shortest JPDA compute time) of the JPDA and BP algorithms.

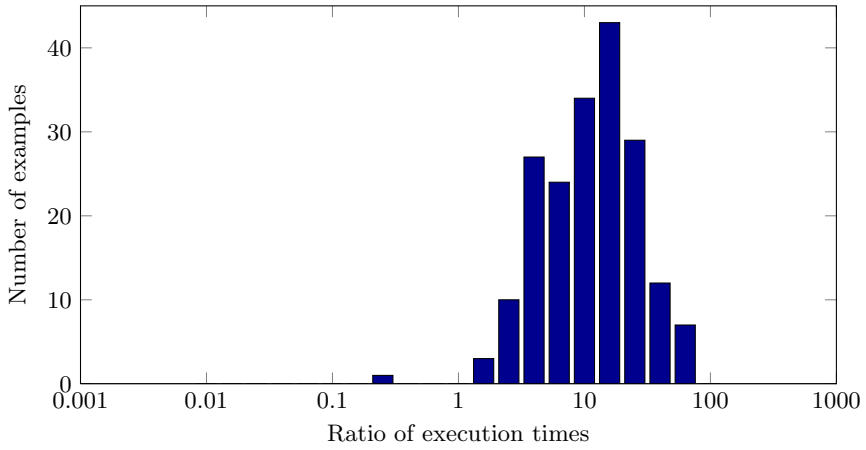

Figure 4: Histogram of the ratio of JPDA to BP compute times. Values greater than 1 imply that BP is faster.

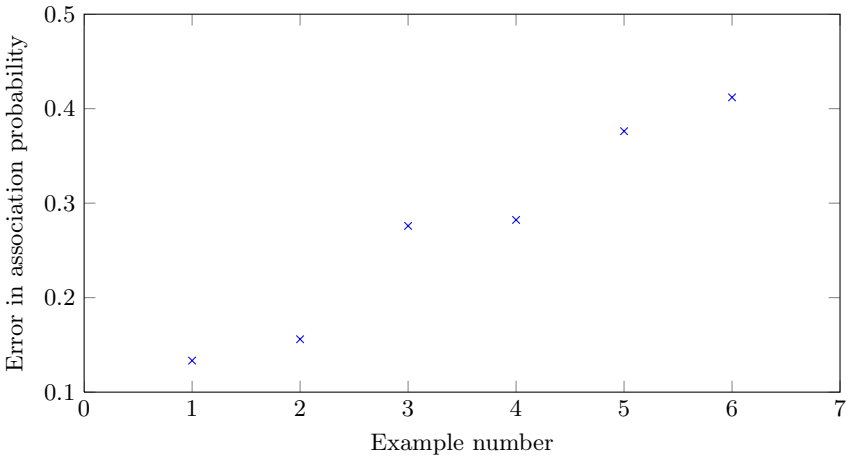

Figure 5: The magnitude of the maximum difference between the BP approximate association probabilities and JPDA in the non-negligible cases (6 out of 192 examples).

there is a single example where the compute time for BP is slower (≈ 5 times) than explicit JPDA calculation. This slow example also corresponds to the least accurate BP approximation.

Here we use a similar metric to [7] to assess the accuracy of the association probabilities. For each example we find the maximum difference between the BP calculated marginal probabilities and those calculated by JPDA. In the majority of cases the differences are very small, less than 0.01, which we assume to be negligible. There are, however, six cases (about 3% of the total) which have larger errors. Each of these errors is shown in Figure 5. The largest error is a difference in probability of 0.41. This corresponds to the difference between an object being assigned roughly evenly to two measurements (JPDA) and the object being assigned to a single measurement (BP). It is the subject of ongoing analysis to determine the effect of these differences on overall track accuracy.

In all but one of the cases with high error the problem is small (3 or 4 objects assigned to 2 or 3 measurements) and the computational expense in calculating these examples exactly is similar to BP. However in the largest case (13 objects being assigned to 7 measurements) the error is just 0.13 while BP is roughly 100 times faster than JPDA. Although there are too few instances in this simulation to make a conclusive judgement, these results suggest that a pragmatic approach would be to apply JPDA to small association problems, where there is little compuational advantage in BP, and apply a BP approximation to large association problems where there can be significant computational gains.

Recent research [13] has shown that the fractional free energy proposed in [14] can provide approximate marginal probabilities with improved accuracy in comparison to BP for problems with high probability of detection and low false alarm rate. Preliminary work has shown that the worst-case error can be reduced from 0.41 to 0.002 using this method (below our threshold for negligible difference), although the method in [13] is somewhat slower than BP for the problem of interest. Rapid solution of problems with this formulation is a topic of ongoing research.

6. CONCLUSIONS AND FURTHER WORK

This paper has given a brief introduction to the constrained admissible region multiple hypothesis filter (CAR-MHF) for initialising and maintaining orbital estimates from angle and angle-rate measurements. Joint probabilistic data association (JPDA) has been described as an approach to deal with measurement-to-object association ambiguity within CAR-MHF. As JPDA can be a computational bottleneck in CAR-MHF, a method of approximating the JPDA calculations has been evaluated, based on belief propagation (BP) in a graphical model (see Figure 2). Comparisons of JPDA and BP methods on a simulated data set have shown that in the majority of cases BP offers a significant advantage in computation time (roughly 20 times faster on average) with negligible difference in the resulting association probabilities. The results suggest that the small number of cases where BP produced a higher error could be largely avoided by using explicit JPDA for small problems and limiting the use of BP to large problems, where it displays the most benefit.

We have two ongoing areas of research related to data association within CAR-MHF. The first of these is to analyse the effect of the BP approximations on the track quality of larger simulated data sets. While admitting that BP is an approximation, track quality is the ultimate measure of system performance, regardless of the data association scheme. The second area is in the investigation of alternative schemes for approximating association probabilities. If our track quality analysis concludes that the BP approximations are insufficient then there are other options that can be explored, such as the previously mentioned fractional free energy approach [13].

REFERENCES

[1] K. J. DeMars, M. K. Jah, and P. W. Schumacher, "Initial orbit determination using short-arc angle and angle rate data," *IEEE Transactions on Aerospace and Electronic Systems*, vol. 48, pp. 2628–2637, July 2012.

[2] K. J. DeMars and M. K. Jah, "Probabilistic initial orbit determination using Gaussian mixture models," *Journal of Guidance, Control and Dynamics*, vol. 36, pp. 1324–1335, Sep-Oct 2013.

[3] J. Stauch, M. Jah, J. Baldwin, T. Kelecy, and K. Hill, "Mutual application of joint probabilistic data association, filtering, and smoothing techniques for robust multiple space object tracking," in *Proceedings of the AIAA/AAS Astrodynamics Specialist Conference*, no. AIAA-2014-4365, Aug. 2014.

[4] Y. Bar-Shalom and X. R. Li, *Multitarget-Multisensor Tracking: Principles and Techniques*. YBS Publishing, 1995.

[5] J. Collins and J. Uhlmann, "Efficient gating in data association with multivariate Gaussian distributed states," *IEEE Transactions on Aerospace and Electronic Systems*, vol. 28, pp. 909–916, July 1992.

[6] J. L. Williams and R. A. Lau, "Data association by loopy belief propagation," in *Proceedings of the 13th International Conference on Information Fusion*, (Edinburgh, UK), pp. 1–8, July 2010.

[7] J. L. Williams and R. A. Lau, "Convergence of loopy belief propagation for data association," in *Proceedings of the 13th International Conference on Information Fusion*, (Edinburgh, UK), pp. 175–180, July 2010.

[8] J. L. Williams and R. A. Lau, "Approximate evaluation of marginal association probabilities with belief propagation," *arXiv:1209.6299 [cs]*, Sept. 2012.

[9] E. A. Wan and R. van der Merwe, "The unscented Kalman filter," in *Kalman Filtering and Neural Networks* (S. Haykin, ed.), ch. 7, John Wiley and Sons, 2001.

[10] H. W. Sorenson and D. L. Alspach, "Recursive Bayesian estimation using Gaussian sums," *Automatica*, vol. 7, pp. 465–479, July 1971.

[11] B. D. O. Anderson and J. B. Moore, *Optimal Filtering*. Prentice-Hall, 1979.

[12] B. Chen and J. K. Tugnait, "Tracking of multiple maneuvering targets in clutter using IMM/JPDA filtering and fixed-lag smoothing," *Automatica*, vol. 37, pp. 239–249, Feb. 2001.

[13] J. L. Williams, "Interior point solution of fractional Bethe permanent," in *Proceedings of the IEEE Workshop on Statistical Signal Processing*, July 2014.

[14] M. Chertkov and A. B. Yedidia, "Approximating the permanent with fractional belief propagation," *Journal of Machine Learning Research*, vol. 14, pp. 2029–2066, 2013.